European Journal of Radiology Open 6 (2019) 320–329

Contents lists available at ScienceDirect

European Journal of Radiology Open

journal homepage: www.elsevier.com/locate/ejro

Atypical presentations of parathyroid gland pathology: A pictorial review

Xin-Ying Kowa[a,1,*], Polly Richards[a], Mona Waterhouse[c], Laila Parvanta[b], Ashok Adams[a]

[a] Department of Radiology, St Bartholomew's Hospital, West Smithfield, London, EC1A 7BE, UK
[b] Department of Endocrine Surgery, St Bartholomew's Hospital, West Smithfield, London, EC1A 7BE, UK
[c] Department of Endocrine and Metabolic Medicine, St Bartholomew's Hospital, West Smithfield, London, EC1A 7BE, UK

ARTICLE INFO

Keywords:
Parathyroid gland enlargement
Cystic parathyroid gland
Ectopic intrathyroidal parathyroid gland
Parathyroid gland haemorrhage
Non-Enhancing parathyroid glands
Hyperparathyroidism jaw tumour syndrome

ABSTRACT

Primary hyperparathyroidism is associated with significant morbidity and mortality. It is in this day and age, an eminently treatable condition which relies heavily on preoperative imaging to localise enlarged parathyroid glands. The imaging appearances of parathyroid gland enlargement are varied; this paper seeks to address some of its more unusual manifestations with an emphasis on its atypical enhancement patterns, mimics and associations. An enlarged glands may also present as an 'incidentaloma' in head and neck imaging performed for entirely different indications, or as part of sporadic or familial syndrome. Radiologists are in a good position to expedite the relevant investigations and curative treatment, and knowledge of the spectrum of imaging appearances is crucial.

1. Introduction

Primary hyperparathyroidism is biochemically defined by hypercalcaemia and elevated or inappopriately normal parathyroid hormone levels as a result of parathyroid gland overactivity. Whilst 'stones, bones, groans and moans' typifies the classical textbook presentation, the systemic manifestations are varied and there are a myriad of clinical presentations. In the conventional outpatient setting, imaging plays an integral part in identifying parathyroid gland enlargement and accurate pre-treatment localisation of potential surgical candidates to enable resection via a minimally-invasive approach. In our institution, concordance between two different imaging modalities is sought prior to surgical intervention. However, the appearance of parathyroid gland enlargement and pathology can be varied and the radiologist should be aware of the spectrum of atypical presentations highlighted in this paper. The spectrum of typical and atypical imaging appearances is presented with potential pitfalls encountered in our practice in a tertiary centre. On describing parathyroid gland pathology in our institution the term *parathyroid gland enlargement* is used in preference to *parathyroid gland adenoma*, as functioning hyperplastic glands and parathyroid carcinoma can be indistinguishable on clinical and imaging examinations [1].

2. Conventional imaging techniques and the classic manifestations of parathyroid gland enlargement

A number of imaging modalities are available for the investigation of hyperparathyroidism and detection of parathyroid gland enlargement.

2.1. Ultrasonography

Ultrasound is an excellent non-invasive imaging modality for examination of the superficial structures of the neck. Scanning is best performed with a high frequency linear-array transducer probe with greyscale imaging used in conjunction with colour and power Doppler. Candidates for parathyroid gland enlargement are typified by their hypoechoic appearance (this is relative to thyroid parenchyma and due to compact cellularity of the lesion), ovoid or cigar-shaped morphology and classic location(s) with lesions most commonly sited in the retrothyroid (> 90%) position at the level of the cricothyroid junction or in the infrathyroid (4%) position (Fig. 1). Peripheral vascularity and a feeding vessel (the 'polar vessel' sign) can be seen on colour Doppler although in the authors' experience this can be difficult to assess in lesions in close proximity to the carotid vessels and inherent pulsation artefact [2].

* Corresponding author.
E-mail addresses: xin-ying.kowa@nhs.net (X.-Y. Kowa), polly.richards2@nhs.net (P. Richards), waterhouse.mona@nhs.net (M. Waterhouse), laila.parvanta1@nhs.net (L. Parvanta), ashok.adams@nhs.net (A. Adams).
[1] Present address: Imaging Department, University College Hospital, 235 Euston Road, Ground Floor North, London, NW1 2BU, UK

https://doi.org/10.1016/j.ejro.2019.10.001
Received 11 September 2019; Received in revised form 6 October 2019; Accepted 8 October 2019
Available online 08 November 2019

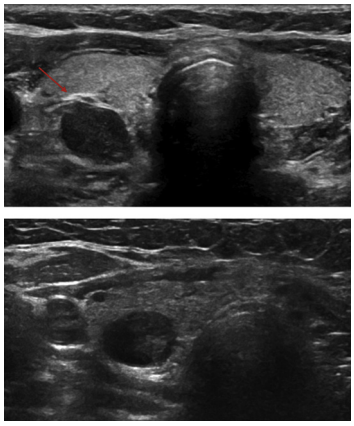

Fig. 1. (a) Classic sonographic appearance and site of an enlarged right-sided parathyroid gland. These are often ovoid and hypoechoic relative to the thyroid parenchyma. Enlarged glands are often situated in a retro-thyroid location and it is important to describe the location(s) of potential candidate(s) in the radiology report (e.g. posterior to the mid-pole of the thyroid) to aid minimally-invasive parathyroidectomy and neck exploration. **(b)** Ultrasound image from a different patient. This is a partly-exophytic U3 (BTA classification) nodule located within the deep aspect of the right thyroid lobe. Both lesions appear similar at first glance however, the subtle fat plane (arrowed) separating thyroid and parathyroid tissue in **(a)** and not appreciated in **(b)** can serve as a useful distinguishing feature.

2.2. Nuclear scintigraphy

Preoperative imaging is performed using technetium-99 m sestamibi radiotracer. The single-radioisotope dual-phase planar imaging technique exploits the differential washout between thyroid and parathyroid tissue. Candidate(s) for parathyroid gland enlargement demonstrate radiotracer retention on delayed image acquisition and in our institution, this is supplemented with single photon emission computed tomography (SPECT) imaging for anatomical localisation of the lesion(s) in 3-dimensional space. False negatives may occur with pre-existing thyroid disease or previous thyroid surgery, necessitating the need for dual-radioisotope dual-phase scintigraphy with thyroid-selective technetium-99 m pertechnetate used in addition to technetium-99 m sestamibi [3]. Radiologists should also be aware of potential false positives as radiotracer can concentrate in nodal (reactive and malignant), salivary and thymic tissue [4] (Fig. 2).

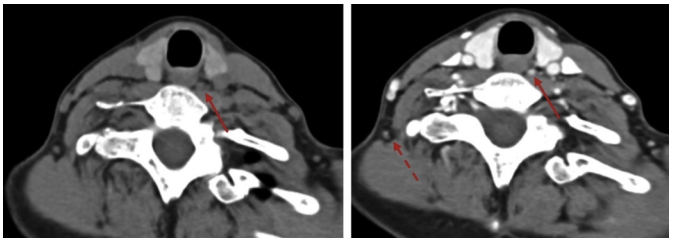

Fig. 3. Axial pre and post-contrast CT images through the neck. The post-contrast images were acquired at 25 s following intravenous contrast administration to coincide with peak enhancement of parathyroid tissue. The images demonstrate the presence of an avidly-arterialising, hypervascular lesion within the left tracheo-oesophageal groove which was deemed to represent a good candidate for an enlarged parathyroid gland (solid arrows). The lesion is hyperattenuating relative to lymphoid tissue (broken arrow) and this differential enhancement is a useful distinguishing feature.

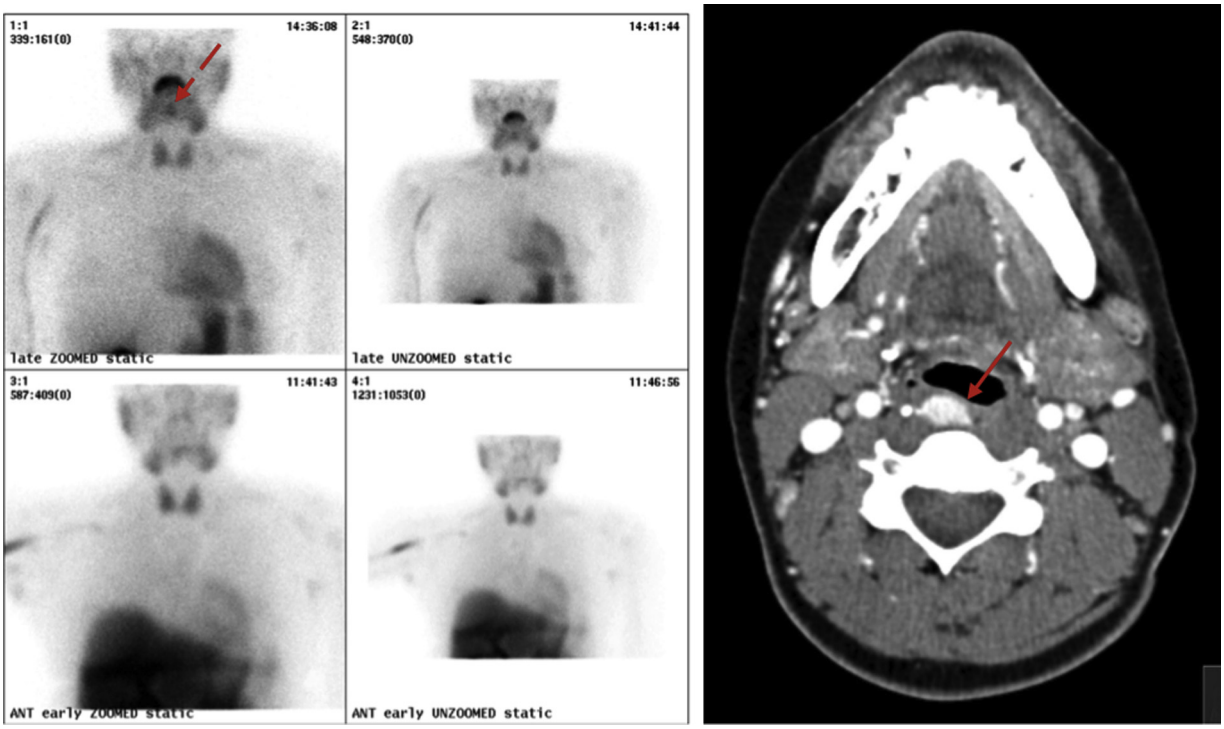

Fig. 2. Retropharyngeal parathyroid gland. **(a)** The Tc-99 m sestamibi study was originally reported as negative for parathyroid gland enlargement. **(b)** An avidly-enhancing focus within the retropharyngeal space at the level of the floor of the mouth (arrow) was described on subsequent CECT. Both sets of images were jointly reviewed by radiologists and nuclear medicine physicians in the endocrine multidisciplinary team meeting. Radiotracer retention on the delayed acquisitions (broken arrow) was identified retrospectively. This case highlights the importance of additional functional and cross-sectional studies for imaging concordance as ultrasound is notoriously limited in its ability to detect ectopic parathyroid tissue. Additionally, potential candidates for parathyroid gland enlargement may be easily overlooked if present in unusual locations or under/over-reported given that delayed Tc-99 m sestamibi washout can be seen in a variety of non-thyroid/parathyroid tissue.

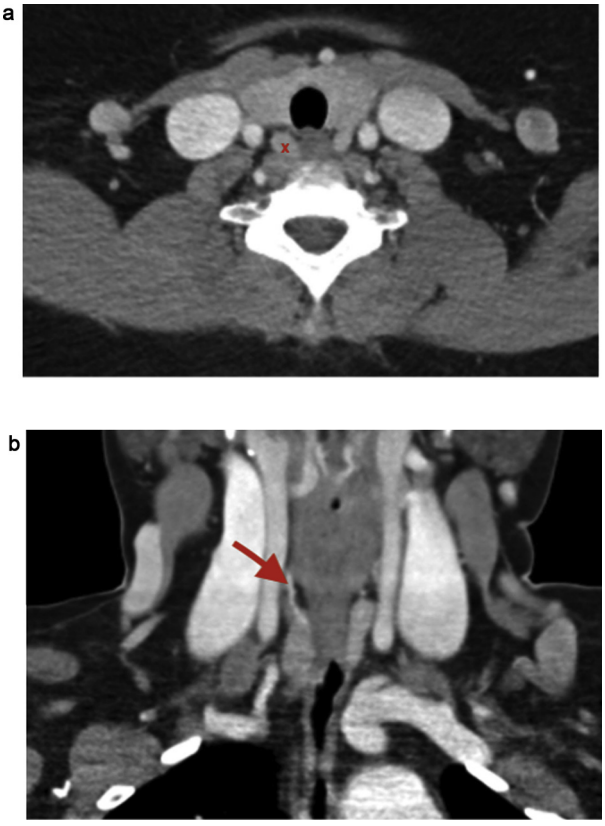

Fig. 4. (a) Axial CECT image demonstrates an enlarged parathyroid gland in the retrothyroid location (x) on the right. There is a further candidate in the mirror-image location within the contralateral neck medial to the left common carotid artery. **(b)** Coronal reformats better demonstrate a feeding artery (arrow) - this is usually a branch of the thyrocervical trunk.

2.3. Cross-sectional imaging

Parathyroid adenomata predominantly derive their arterial supply via the inferior thyroid artery (branch of the thyrocervical trunk) and enlarged parathyroid glands are typically hypervascular lesions demonstrating avid arterial enhancement [5] (Fig. 3). Whilst a vascular pedicle may be identified, its presence is not required for definitive diagnosis (Fig. 4). In our institution, contrast-enhanced computed tomography (CECT) scanning is performed from the skull base down to the level of the carina with images acquired at 25 s to coincide with peak contrast-enhancement of parathyroid tissue in the arterial phase. Additional pre-contrast and delayed imaging can be added, particularly for patients with nodular thyroid disease and in patients who have undergone previous parathyroidectomy surgery.

Multiphase 4D-CT emerged in 2006 [6] as a useful adjunct in parathyroid adenoma localisation and since then, variations on the initially proposed protocol have been developed. In addition to rapid arterialisation, early contrast wash out (relative to thyroid and nodal tissue) demonstrated on delayed acquisitions [7] can provide useful perfusion data and aid in distinguishing parathyroid tissue from adjacent lymph nodes or exophytic thyroid nodules. Additional information offered by 4D-CT however comes at the cost of increased radiation exposure to the patient.

Dynamic and multiparametric MRI techniques have more recently entered into clinical practice in some American and European institutions. This exploits similar principles to 4D-CT and the enhancement and wash out characteristics of parathyroid adenomata (though lipid-rich adenomata have been described to demonstrate more delayed wash out relative to the more cellular lesions). A retrospective study by Nael et al. [8] has reported a high (96%) diagnostic accuracy in adenoma

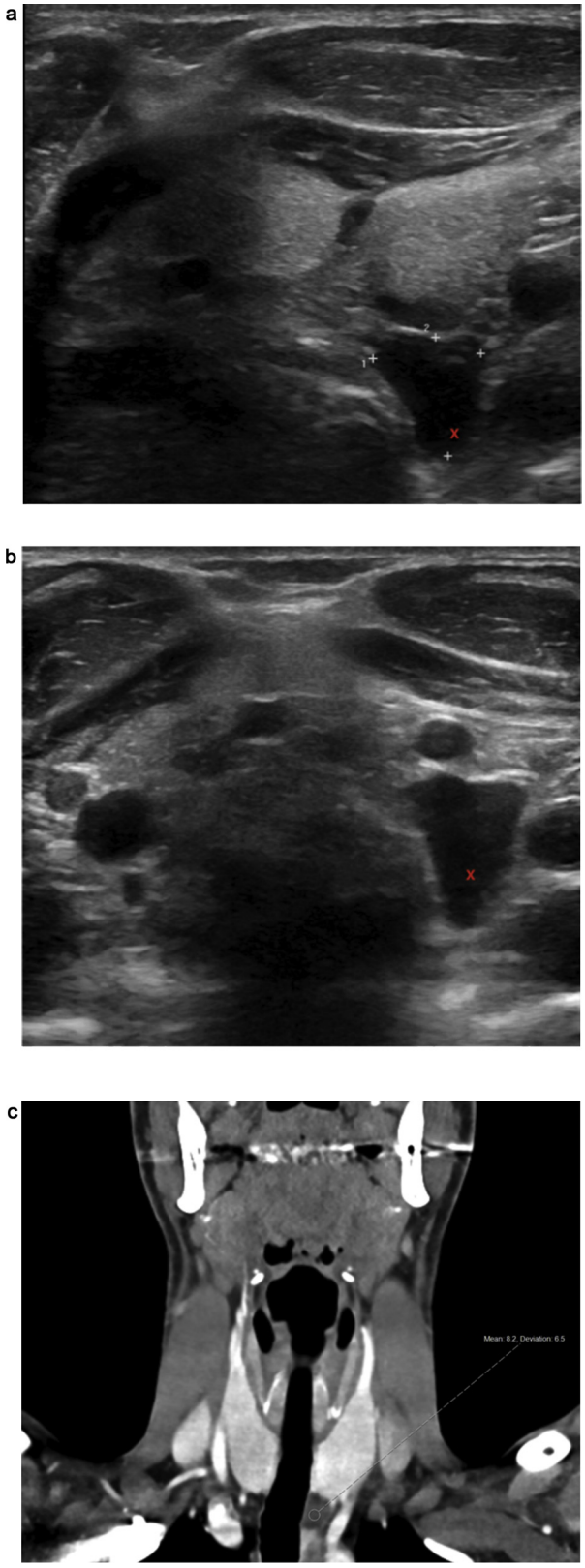

Fig. 5. Cystic parathyroid gland. **(a)** Transverse ultrasound images through level VI demonstrate a cystic lesion (x) posterior to the lower pole of the left thyroid gland and **(b)** extending into level VII of the neck in a patient investigated for primary hyperparathyroidism. Posterior acoustic enhancement was evident and no solid components were identified. The radiologist was confident that this represented a functional parathyroid cyst however, the lower pole of the lesion was not visualised sonographically and CECT was performed for full assessment. (c) Coronal CECT confirms the presence of an enlarged, cystic parathyroid gland (< 10HU in density).

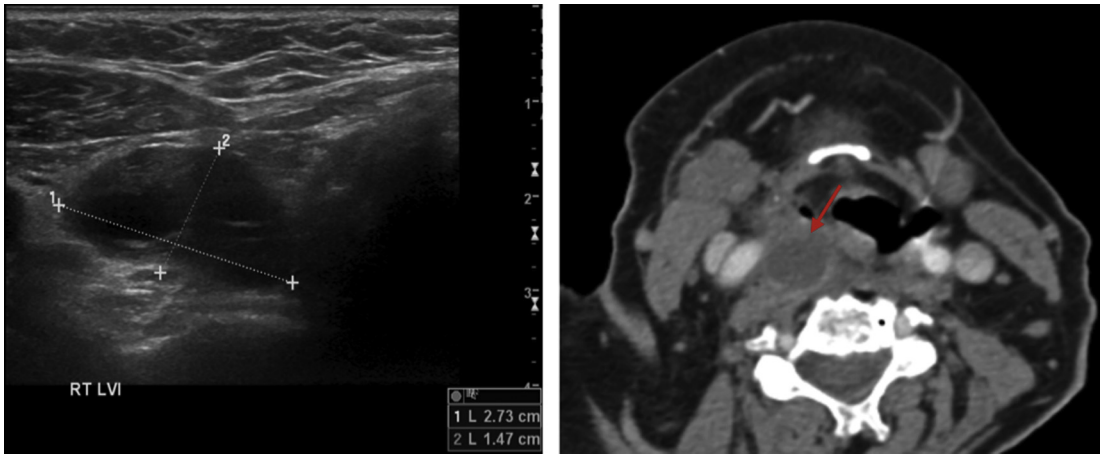

Fig. 6. Ultrasound **(a)** and CECT **(b)** performed for the investigation of primary hyperparathyroidism. The images demonstrate an extra-thyroid, right-sided septated cystic-solid lesion within level VI of the neck and the arrow points to non-dependent, subtle intralesional soft tissue. There is effacement of the right pyriform fossa more superiorly. Fine needle aspiration was unfortunately non-diagnostic and this was subsequently confirmed as an enlarged parathyroid gland following resection and histology. Its complex appearances suggest cystic degeneration or prior haemorrhage into the gland. This case highlights the importance of requesting a parathormone assay at the same time as cytological analysis.

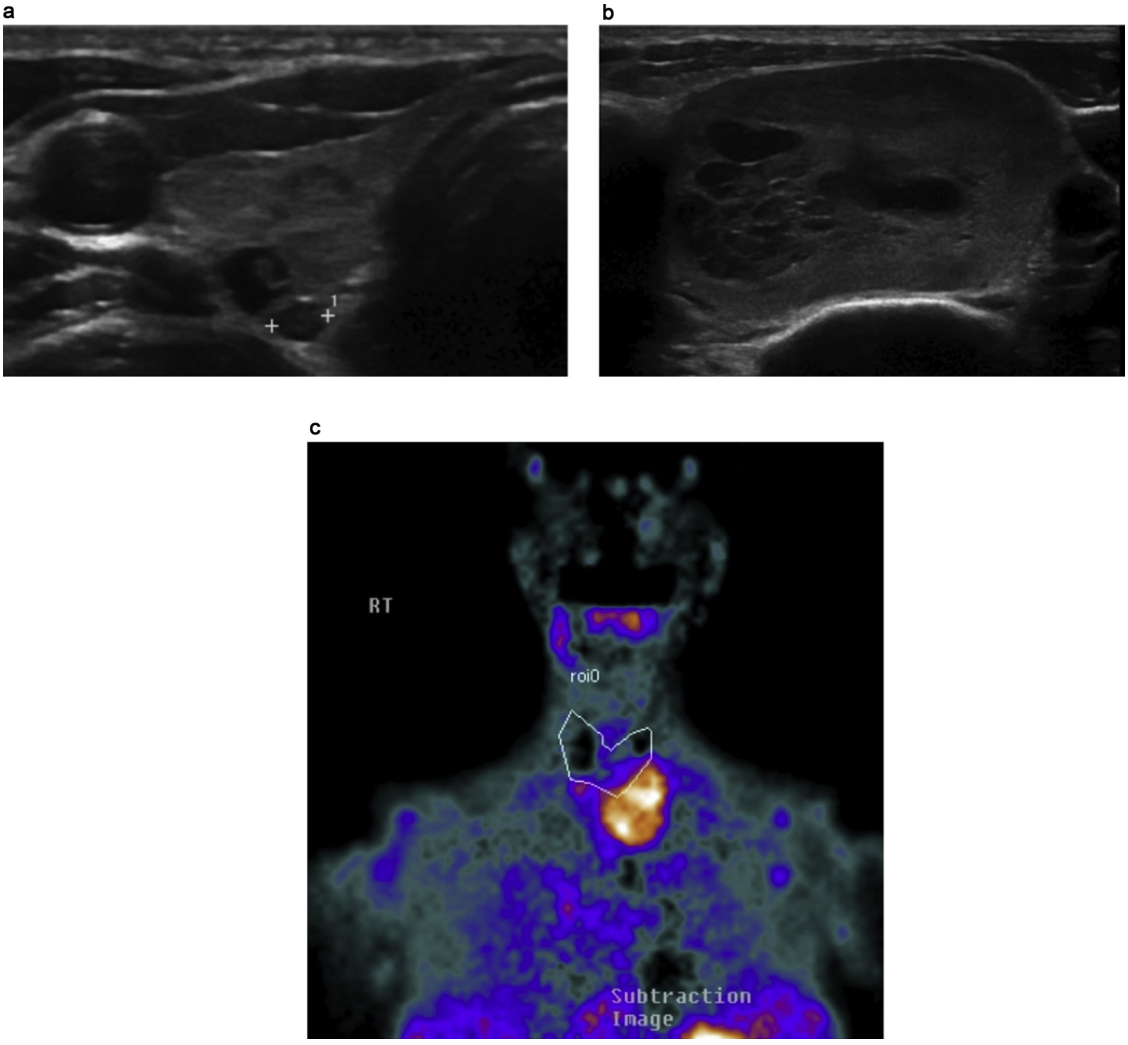

Fig. 7. (a) and **(b)** Sonographic assessment of the neck confirmed the presence of a multinodular goitre; there was marked and asymmetric enlargement and hyperplastic change on the left. A potential candidate for parathyroid gland enlargement was demonstrated on the right and a benign, dominant and partly-exophytic thyroid nodule described on the left. **(c)** Subtraction image from nuclear scintigraphy demonstrates concordance on the right but also raised the possibility of an enlarged left-sided parathyroid lesion. The suspicion of an intra-thyroid parathyroid gland on the left was corroborated on venous sampling.

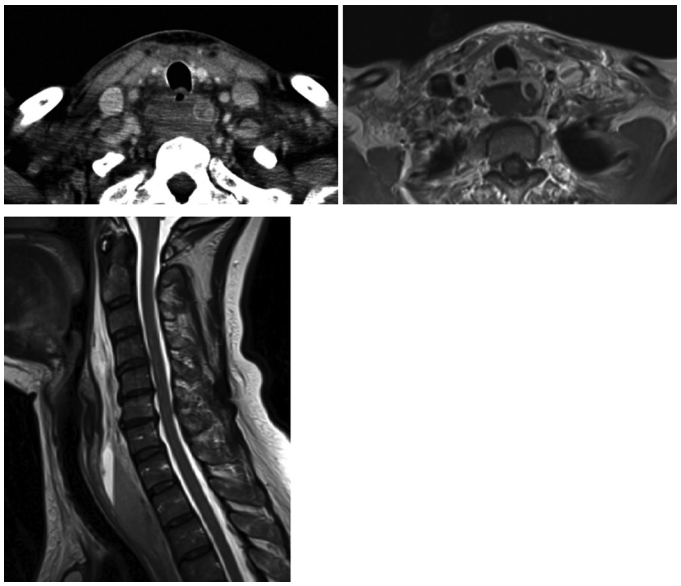

Fig. 8. This patient underwent imaging after presenting to Accident and Emergency with rapid-onset dysphagia, neck and chest pain. **(a)** CECT (ENT soft tissue protocol) showed extensive retropharyngeal haematoma causing compression of the oesophagus and a peripherally-enhancing focus within the left para-oesophageal region. **(b)** and **(c)** The subsequent T1 post-contrast axial image showed a similar finding with layered hyperacute-acute blood products within the retropharyngeal space and better appreciated on the T2 sagittal image. The patient had no history of trauma or underlying coagulopathy to account for this. Follow up ultrasound study identified an enlarged parathyroid gland favouring a ruptured adenoma as the cause for the patient's acute presentation.

Fig. 9. This patient presented to Accident and Emergency following chest pain and stridor. A large, hypoattenuating lesion was seen within the superior mediastinum on CECT. This was inseparable from the upper aerodigestive tract structures, and deviation and compression of the trachea and oesophagus was described. The initial differentials included an underlying lymphoproliferative disorder, bronchogenic malignancy and parathyroid carcinoma (given the abnormal calcium profile). This was resected following multidisciplinary discussion and histology confirmed a haemorrhagic, benign parathyroid adenoma. The apparent non/hypo-enhancement was due to intralesional haematoma.

detection using 3 T scanners, and this has been corroborated by a more recent retrospective study by Ozturk et al [9]. Imaging with MRI and dual-energy 4D-CT (first utilised in 2010) obviates and reduces any radiation concerns, and therefore allows for imaging at multiple time points [10]. Access to this resource remains limited by its cost and availability and moreover, the large field of view required limits both temporal and spatial resolution with increased susceptibility to artefact than CECT particularly in the upper mediastinum.

There are clinical trials that aim to elucidate the potential of fusion MRI and SPECT for the purposes of parathyroid adenomata localisation [11].

2.4. Parathyroid venous sampling

There is a role for venous sampling via fluoroscopic-guided invasive catheter venography albeit in a select patient cohort. Its main utility is as a problem-solving tool in cases of non-localisation, discordant findings on previous imaging examinations and where there is persisting or recurrent primary hyperparathyroidism despite prior surgery. The principle relies on selective catheterisation of the parathyroid gland draining veins and comparison of intravenous parathormone levels obtained from these vessels (2–3 millilitres blood sample required per site) against a reference i.e. parathormone level from the subclavian vessels. Whilst this has been proven to be the most sensitive test for ectopic or missed lesions, its invasive nature, average procedure time of 90 min [12] and inherent risks render it less desirable as a tool for initial investigations [13].

3. The spectrum of atypical imaging appearances of parathyroid gland enlargement

3.1. Cystic parathyroid glands

Parathyroid gland enlargement may present as purely cystic lesions in 3% of cases [14], and cystic adenomata have also been referred to as functional parathyroid cysts in this context [15]. The cystic appearance is commonly due to internal necrosis within a hyperplastic gland, degeneration of an adenoma or secondary to intralesional haemorrhage. Cystic parathyroid adenomata may be simple in appearance with through transmission demonstrated on ultrasound **(**Fig. 5**)**, or display more complex sonographic features with internal septae and soft tissue components **(**Fig. 6**)**. The largest dimension of adenomata is usually along its craniocaudal axis, and an echogenic plane separating adenomata from the thyroid gland may be evident as may a feeding vessel on Doppler [15]. The presence of these features can increase the diagnostic confidence especially when differentiating adenomata from exophytic thyroid nodules. The cystic components of these lesions return fluid attenuation on CECT. Fusion studies i.e. SPECT and positron emission tomography-CT (PET-CT) may depict these as 'cold' lesions [14], thus mandating fine needle aspiration (FNA) for biochemical analysis and characterisation with alternate imaging modalities. Aspirated cyst fluid is clear and colourless, but may be straw-coloured or turbid in a fifth of cases [14]. Cystic adenomata yield a similar biochemical profile to their more solid-appearing counterparts with raised levels of parathormone from FNA and needle washout for dedicated parathormone assay.

A differential for cystic parathyroid gland enlargement includes non-functional parathyroid cysts. These have been regarded by some as a distinct entity from functional parathyroid cysts (i.e. cystic adenomata) given their disparate embryologic origin with the presence of an epithelial lining and lack of adenomatous change on histology [15]. Imaging alone cannot distinguish between these entities although retrospective analysis has shown that 'true' and non-functional cysts tend to present at a larger size (investigated due to their compressive effects) as patients are otherwise asymptomatic and eucalcaemic. This is further complicated as parathyroid carcinoma can also present as a cystic parathyroid mass [14]. A high index of suspicion of parathyroid cysts is required as this is more commonly the presentation of cystic metastatic

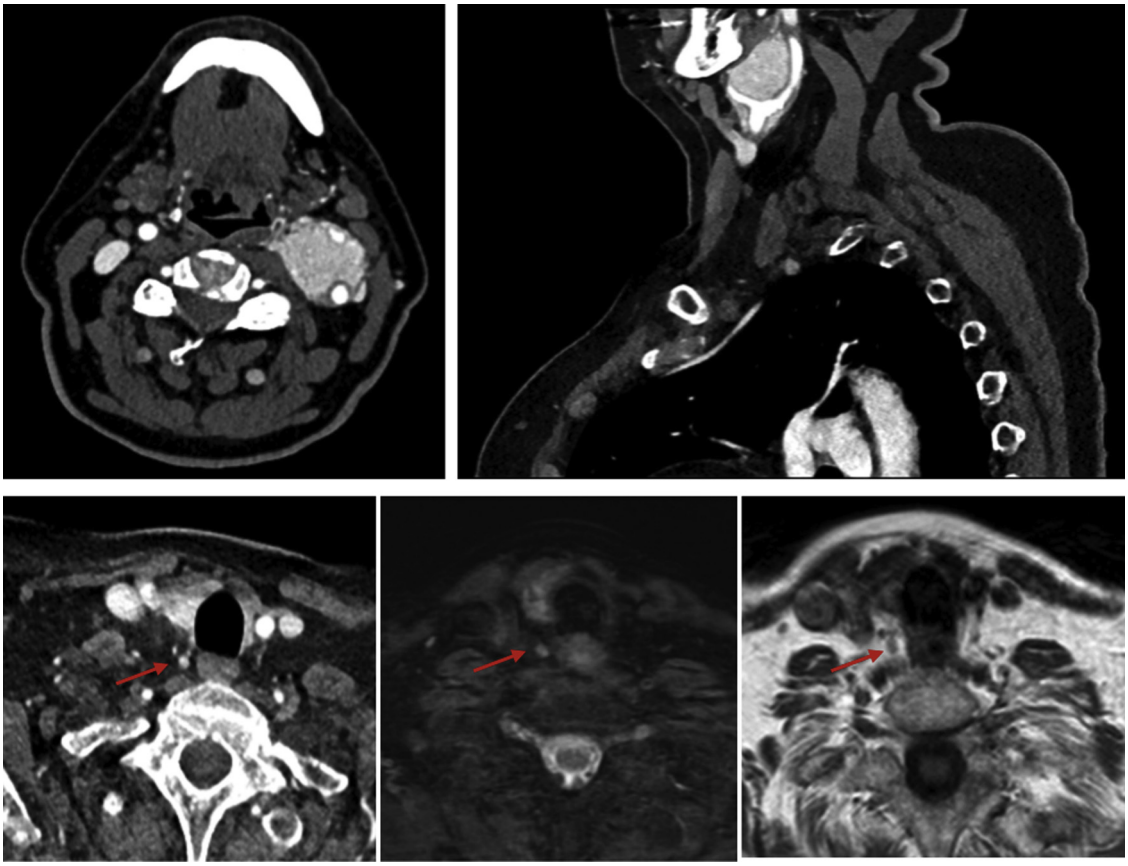

Fig. 10. CECT and MRI images from a young woman undergoing screening for succinyl dehydrogenase (SDH) mutation. SDH mutations are germline mitochondrial defects which place patients at increased risk of developing multi-system neoplasms including paragangliomas in the head and neck region. In our institution, screening involves non-contrast whole body MRI (neck, thorax, abdomen and pelvis). **(a)** and **(b)** A left-sided carotid body tumour was found on CECT. **(c)** A millimetric hypervascular focus was seen in the right tracheo-oesophageal groove on the axial images. This was confirmed to represent an enlarged parathyroid gland on further assessment and this was found to be present on historic screening MR imaging; **(d)** parathyroid tissue is typically T2/STIR-hyperintense and **(e)** T1-isointense. These lesions can be difficult to detect due to their small size and similar signal characteristics to nodal tissue.

lymph nodes, branchial cleft cysts and thyroglossal duct cysts.

3.2. Intra-thyroidal parathyroid glands

Ectopic glands are seen in 16% of cases investigated for hyperparathyroidism and lesions may be found from the level of the angle of the mandible to the mediastinum [16].

Intra-thyroid candidates for parathyroid gland enlargement are an uncommon entity with a reported incidence between 1–7% of parathyroidectomy cases depending on the definition of 'intra-thyroid' in the literature. Partly-enveloped parathyroid lesions (> 50% surrounded by thyroid tissue) and those completely embedded in the thyroid gland have varyingly been described as intra-thyroid [17]. The parathyroid glands are embryologically derived from the 3rd and 4th pharyngeal pouches (the former also giving rise to the lateral anlage of the thyroid gland) and undergo varying degrees of descent throughout gestation. This shared embryological origin and lack of capsular fixation may facilitate aberrant migration and the subsequent engulfment of parathyroid tissue within the thyroid gland [16]. Identification and localisation of intra-thyroid parathyroid lesions is further complicated in the setting of a multinodular thyroid gland. Nodules of thyroid origin are less likely to demonstrate a polar feeding vessel hence solid nodules that are hypoechoic relative to thyroid parenchyma, taller-than-wide, hypervascular and possess a polar feeding vessel should be viewed as potential candidates for parathyroid gland enlargement [18]. Fine needle aspirates should be performed at this point and sent for both cytology and parathormone assay. **(**Fig. 7**)**

3.3. Parathyroid gland haemorrhage

Capps et al. described the first case of parathyroid haemorrhage in 1934 [19] and there have since been literature case reports documenting this relatively uncommon presentation of parathyroid gland enlargement. Rupture and haemorrhage of a parathyroid lesion (also referred to as parathyroid apoplexy) is the result of necrosis and involution. The thin capsule surrounding the gland predisposes to extracapsular dissection of haematoma into the deep neck spaces and mediastinum [20]. Patients can present acutely with airway compromise and sudden neck swelling as well as neck and/or chest bruising, dysphagia and dysphonia (the result of compression on the oesophagus, vagus or recurrent laryngeal nerve). Serum biochemistry can be very variable with patients presenting in hypercalcaemic crises, in eucalcaemic or hypocalcaemic states; the latter two are thought to be the consequence of parathyroid gland infarction [21]. Whilst spontaneous gland infarction can lead to remission of primary hyperparathyroidism, this does not always equate to an auto-parathyroidectomy as biochemical evidence of recurrent disease have been reported, likely secondary to remnant parathyroid tissue [20].

In this acute setting, patients are likely to have undergone a contrast-enhanced CT neck which may not identify parathyroid gland arterial enhancement as this is in our institution, a single phase acquisition triggered at 90 s to allow for opacification of vessels and contrast uptake by the soft tissues. An underlying parathyroid lesion may not always be seen on initial CECT in the setting of parathyroid gland haemorrhage [22]. The radiologist is likely to encounter extensive

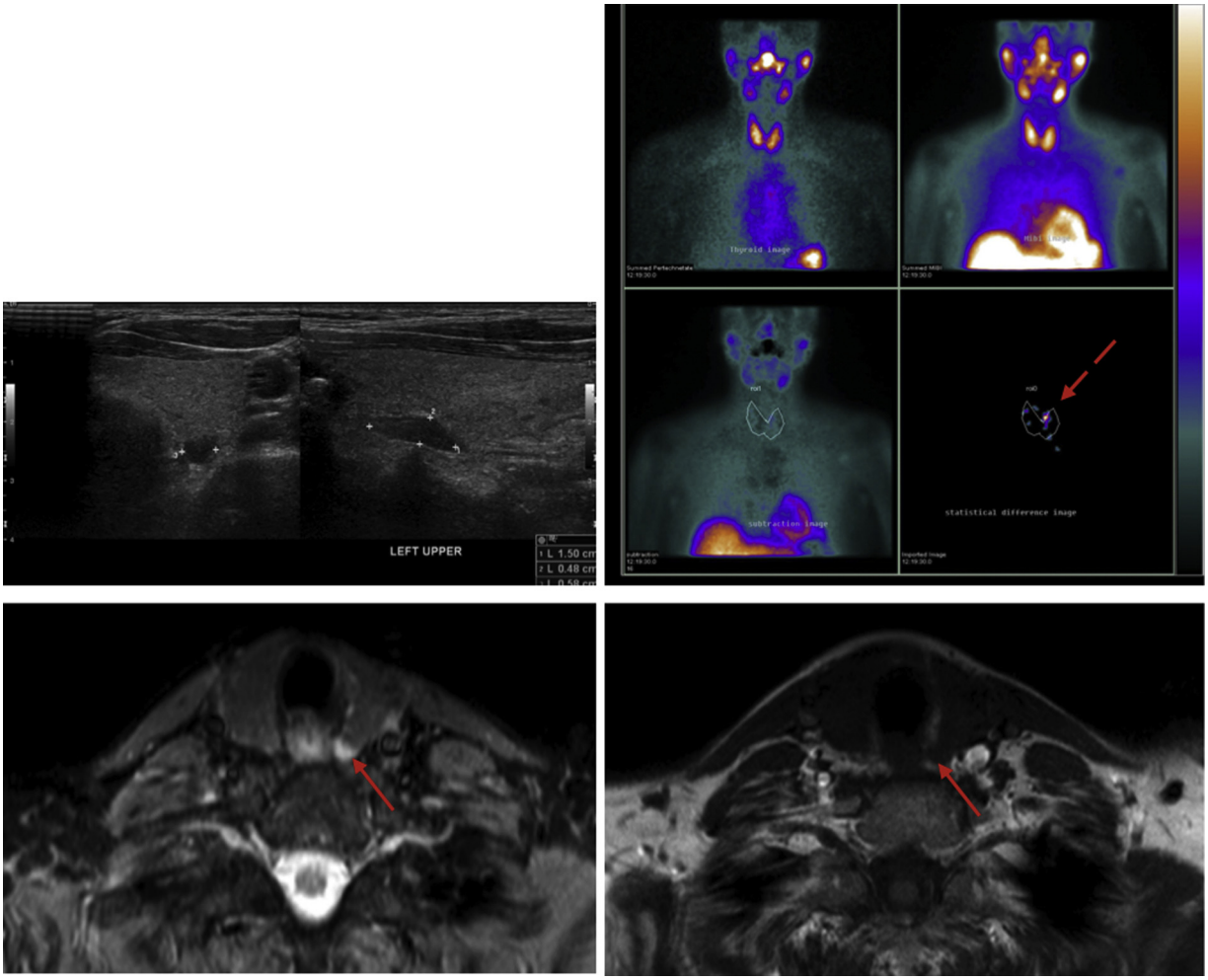

Fig. 11. Images from a different patient who underwent **(a)** sonographic and **(b)** scintigraphic assessment for primary hyperparathyroidism - these confirmed an enlarged parathyroid gland posterior to the upper pole of the left thyroid lobe. Review of prior MR images performed for SDH mutation screening revealed the presence of a cigar-shaped **(c)** T2/STIR-hyperintense and **(d)** T1-hypointense lesion (arrowed) which corresponded to the solitary, functional parathyroid adenoma.

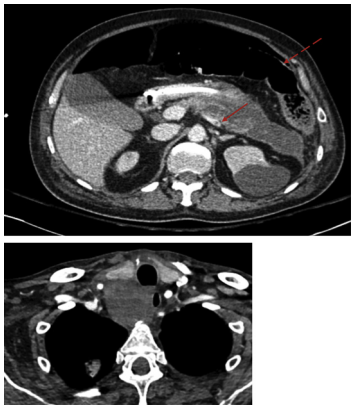

Fig. 12. CECT performed for an intensive care patient who had been admitted with necrotising pancreatitis. **(a)** Imaging through the abdomen demonstrated extensive, loculated peripancreatic fluid collections and splenic vein thrombosis (arrow) complicated by hollow viscus perforation (broken arrow). An underlying parathyroid carcinoma was suspected as the serum calcium levels were found to be > 10x the upper limit of normal. **(b)** Imaging through the neck and chest demonstrated a locally-invasive right-sided parathyroid carcinoma (confirmed on histology) invading the posterior tracheal wall and the posterolateral wall of the oesophagus. Note the very similar imaging appearances between this case and Fig. 10. Focal right upper lobe consolidation was also noted.

haematoma in the neck and upper mediastinum spanning multiple fascial spaces and absent enhancing soft tissue components due to involution/necrosis. CECT can at the same time exclude the presence and complications of ingested foreign body [23] - this being a common presentation of dysphagia and odynophagia **(**Fig. 8**)**.

3.4. Poorly and non-enhancing parathyroid gland enlargement

Enlarged parathyroid glands do not always conform to the aforementioned enhancement criteria. A recent retrospective study published by Bahl et al. in 2015 established measurable enhancement in all the parathyroid lesions they examined and elucidation of three distinct enhancement-washout patterns [24]. A subsequent retrospective study by Goroshi et al. put forth a percentage enhancement cut-off value of ≥128.9% as being 95.8% sensitive and 100% specific for parathyroid adenomata or glandular hyperplasia [25]. There is a paucity of published data relating to non-enhancing lesions but it has been proposed that false negatives arise as a result of intralesional haemorrhage or fibrosis **(**Fig. 9**)**. Prior thyroid surgery, thyroiditis, the presence of a multinodular goitre or variations in patients' cardiovascular function may also alter the regional vascular supply resulting in atypical enhancement characteristics [7]. Even though the aforementioned dynamic imaging techniques allow for good characterisation, the use of single-bolus single-phase (our current and preferred technique) remains prevalent in the United Kingdom given their lower radiation doses. Radiologists should be wary of reporting concordance or non-

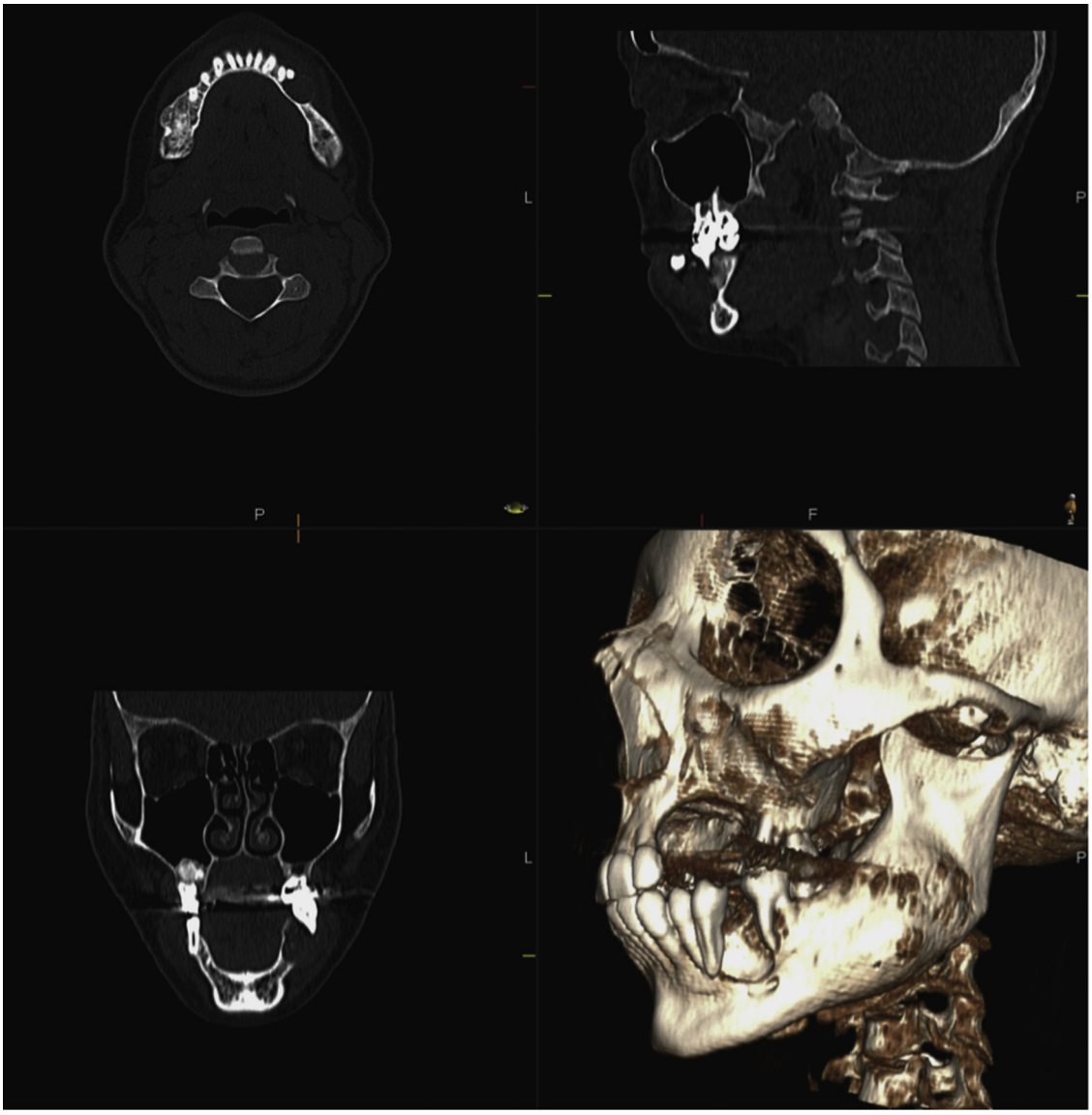

Fig. 13. NCCT (non-contrast CT) multiplanar reconstructions and 3D-rendering of a left mandibular non-ossifying fibroma. The expansile, lucent lesion has remodelled and thinned the mandibular buccal cortex. Whilst it is intimately related to the roots of LL6 and LL7, there is no associated root resorption.

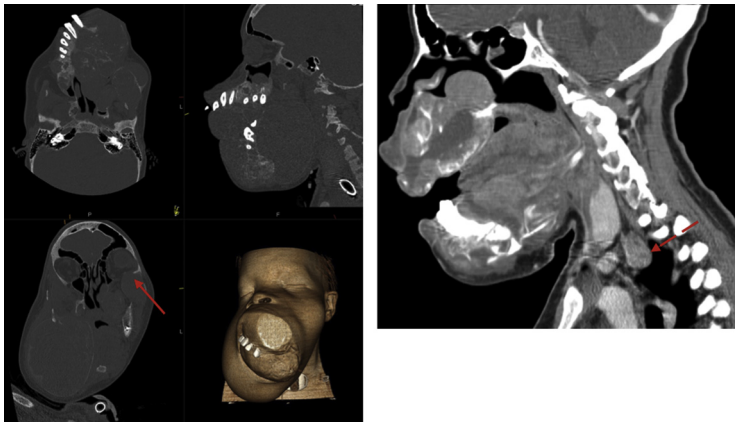

Fig. 14. This is a more extreme case of hyperparathyroidism jaw tumour syndrome. **(a)** Multiplanar CT reconstructions and volume-rendered image demonstrate multiple craniofacial fibromas and significant facial deformity. There is extensive involvement of the maxilla and mandible, with varying degrees of intralesional matrix mineralisation seen. There is encroachment of the left orbital floor (arrow) with a resultant left-sided proptosis. A tracheostomy is in situ. **(b)** An enlarged parathyroid gland was seen on coronal reformats (broken arrow).

concordance when comparing ultrasound, scintigraphic and CT imaging as it may not be possible to reliably differentiate between parathyroid tissue demonstrating atypical delayed enhancement, hypo- or non-enhancement and its mimics (notably thyroid and nodal tissue) especially when images have been acquired at a single time point.

3.5. Incidental detection of parathyroid gland enlargement on MRI

MRI has been utilised for parathyroid adenoma localisation since the 1980s [26] but are not part of routine clinical practice in centres across the United Kingdom for a variety of reasons. In addition, radiologists may encounter potential candidates for parathyroid gland enlargement as 'incidentalomas' during routine head and neck and cervical spine imaging, and may be able to expedite investigations for hyperparathyroidism (Figs. 10 and 11). Parathyroid adenomata are characterised by their hypointense or isointense signal on T1-weighted imaging, T2-hyperintensity and enhancement on post-gadolinium sequences [2]. As with CECT imaging, variable enhancement has been described in sub-solid lesions and with the presence of intralesional fibrosis. Lymph nodes may have similar appearances and care must be taken during image interpretation.

3.6. Hyperparathyroidism jaw tumour syndrome

Multiple endocrine neoplasia (MEN types 1 and 2a) is the well-recognised familial condition associated with the development of parathyroid hyperplasia. Both general and dental radiologists' should also be aware of hyperparathyroidism jaw tumour syndrome as a further cause of parathyroid gland enlargement in young patients with asynchronous, recurrent or multi-glandular disease, and a relevant family history. This is a rare autosomal dominant syndrome arising due to mutations of the HRPT2 tumour suppressor gene on chromosome 1, with approximately 200 cases described in the literature [27].

In addition to the development of adenomata, the risk of parathyroid carcinoma is also significantly increased in this cohort of patients at 15% [28] as opposed to an incidence of 0.005% in the general population. Whilst sonographic, cross-sectional and scintigraphy imaging features early in the disease process are similar to that of benign parathyroid gland enlargement, intravenous parathormone levels are considerably elevated in functional carcinomas (five to ten times the upper limit of normal). Frank invasion of adjacent soft tissues and vasculature within the neck, upper aerodigestive tract and mediastinum are evident later in the disease process, with local recurrence or metastasis (via lymphatic and haematogenous routes primarily to cervical nodes, lungs, liver or skeleton) predicting a poor prognosis [29] (Fig. 12).

Along with parathyroid lesions there are a constellation of benign and malignant craniofacial and urogenital tract lesions that can be present in this syndrome secondary to the underlying genetic defect.

Craniofacial ossifying fibromas and its variants may be seen on a background of hypercalcaemia-related osseous abnormalities. These are distinct from brown tumours and do not regress following parathyroidectomy. Lesions may be small and detected incidentally on clinical examination or dental imaging, and the characteristic appearance is that of a well-defined lucent lesion with sclerotic borders (Fig. 13). These fibro-osseous lesions may be solitary or multiple, uni or multilocular or demonstrate varying degrees of internal matrix mineralisation. Larger lesions can cause significant craniofacial deformity and morbidity given their locally aggressive nature [30] (Fig. 14).

Benign, premalignant and malignant tumours of the urinary tract e.g. benign cysts and hamartomas, papillary renal cell carcinomas and adult-onset Wilm's tumours are associated with HRPT2 mutations [31]. A spectrum of uterine pathologies has been described in affected females ranging from benign leiomyoma growth and adenomyosis to development of malignant adenosarcomas, with patients presenting with menorrhagia and impaired fertility [32].

4. Conclusion

The clinical and imaging features of primary hyperparathyroidism can vary and this paper serves to highlight the atypical presentations of parathyroid gland pathology from an imaging perspective. These presentations are uncommon but they are important to identify and thus guide further investigation of underlying parathyroid gland pathology given the recognised mortality and morbidity from hypercalcaemia and the associated cancer syndromes.

Declaration of Competing Interest

Not applicable.

References

[1] J.P. Bilezikian, L. Bandeira, A. Khan, N.E. Cusano, Hyperparathyroidism, lancet lond. Engl. 391 (2018) 168–178, https://doi.org/10.1016/S0140-6736(17)31430-7.

[2] N.A. Johnson, M.E. Tublin, J.B. Ogilvie, Parathyroid imaging: technique and role in the preoperative evaluation of primary hyperparathyroidism, AJR Am. J. Roentgenol. 188 (2007) 1706–1715, https://doi.org/10.2214/AJR.06.0938.

[3] J.R. Smith, M.E. Oates, Radionuclide imaging of the parathyroid glands: patterns, pearls, and pitfalls, Radiogr. Rev. Publ. Radiol. Soc. N. Am. Inc. 24 (2004) 1101–1115, https://doi.org/10.1148/rg.244035718.

[4] H.K. Eslamy, H.A. Ziessman, Parathyroid scintigraphy in patients with primary hyperparathyroidism: 99mTc sestamibi SPECT and SPECT/CT, Radiogr. Rev. Publ. Radiol. Soc. N. Am. Inc. 28 (2008) 1461–1476, https://doi.org/10.1148/rg.285075055.

[5] G.J. Randall, P.B. Zald, J.I. Cohen, B.E. Hamilton, Contrast-enhanced MDCT characteristics of parathyroid adenomas, AJR Am. J. Roentgenol. 193 (2009), https://doi.org/10.2214/AJR.08.2098 W139-143.

[6] S.E. Rodgers, G.J. Hunter, L.M. Hamberg, D. Schellingerhout, D.B. Doherty, G.D. Ayers, S.E. Shapiro, B.S. Edeiken, M.T. Truong, D.B. Evans, J.E. Lee, N.D. Perrier, Improved preoperative planning for directed parathyroidectomy with 4-dimensional computed tomography, Surgery 140 (2006) 932–940, https://doi.org/10.1016/j.surg.2006.07.028 discussion 940-941.

[7] J.K. Hoang, W. Sung, M. Bahl, C.D. Phillips, How to perform parathyroid 4D CT: tips and traps for technique and interpretation, Radiology 270 (2014) 15–24, https://doi.org/10.1148/radiol.13122661.

[8] K. Nael, J. Hur, A. Bauer, R. Khan, A. Sepahdari, R. Inampudi, M. Guerrero, Dynamic 4D MRI for characterization of parathyroid adenomas: multiparametric analysis, AJNR Am. J. Neuroradiol. 36 (2015) 2147–2152, https://doi.org/10.3174/ajnr.A4425.

[9] M. Ozturk, A.V. Polat, C. Celenk, M. Elmali, S. Kir, C. Polat, The diagnostic value of 4D MRI at 3T for the localization of parathyroid adenomas, Eur. J. Radiol. 112 (2019) 207–213, https://doi.org/10.1016/j.ejrad.2019.01.022.

[10] O. Gimm, C. Juhlin, O. Morales, A. Persson, Dual-energy computed tomography localizes ectopic parathyroid adenoma, J. Clin. Endocrinol. Metab. 95 (2010) 3092–3093, https://doi.org/10.1210/jc.2010-0386.

[11] Evaluation of MRI and SPECT Fusion Software to Localize Parathyroid Adenomas - Full Text View - ClinicalTrials.gov, (n.d.). April 27, 2011. https://clinicaltrials.gov/ct2/show/NCT00639405. (accessed July 7, 2019).

[12] M. Ikuno, T. Yamada, Y. Shinjo, T. Morimoto, R. Kumano, K. Yagihashi, T. Katabami, Y. Nakajima, Selective venous sampling supports localization of adenoma in primary hyperparathyroidism, Acta Radiol. Open 7 (2018), https://doi.org/10.1177/2058460118760361.

[13] R.W. England, E.B. Geer, A.R. Deipolyi, Role of Venous Sampling in the Diagnosis of Endocrine Disorders, J. Clin. Med. 7 (2018), https://doi.org/10.3390/jcm7050114.

[14] K.L. McCoy, J.H. Yim, B.S. Zuckerbraun, J.B. Ogilvie, R.L. Peel, S.E. Carty, Cystic parathyroid lesions: functional and nonfunctional parathyroid cysts, Arch. Surg. Chic. Ill 1960 (144) (2009) 52–56, https://doi.org/10.1001/archsurg.2008.531 discussion 56..

[15] N.A. Johnson, L. Yip, M.E. Tublin, Cystic parathyroid adenoma: sonographic features and correlation with 99mTc-sestamibi SPECT findings, AJR Am. J. Roentgenol. 195 (2010) 1385–1390, https://doi.org/10.2214/AJR.10.4472.

[16] R. Phitayakorn, C.R. McHenry, Incidence and location of ectopic abnormal parathyroid glands, Am. J. Surg. 191 (2006) 418–423, https://doi.org/10.1016/j.amjsurg.2005.10.049.

[17] H. Mazeh, G. Kouniavsky, D.F. Schneider, K.I. Makris, R.S. Sippel, A.P.B. Dackiw, H. Chen, M.A. Zeiger, Intrathyroidal parathyroid glands: small, but mighty (a Napoleon phenomenon), Surgery 152 (2012) 1193–1200, https://doi.org/10.1016/j.surg.2012.08.026.

[18] M.T. Heller, L. Yip, M.E. Tublin, Sonography of intrathyroid parathyroid adenomas: are there distinctive features that allow for preoperative identification? Eur. J. Radiol. 82 (2013), https://doi.org/10.1016/j.ejrad.2012.08.001 e22-27.

[19] R.B. Capps, Multiple parathyroid tumors with massive mediastinal and subcutaneous hemorrhage, Am. J. Med. Sci. 188 (1934) 800–804, https://doi.org/10.1097/00000441-193412000-00007.

[20] W.B. Chan, C.C. Chow, A.D. King, V.T. Yeung, J.K. Li, W.Y. So, C.S. Cockram, Spontaneous necrosis of parathyroid adenoma: biochemical and imaging follow-up for two years, Postgrad. Med. J. 76 (2000) 96–98, https://doi.org/10.1136/pmj.76.892.96.

[21] A. Garrahy, D. Hogan, J.P. O'Neill, A. Agha, Acute airway compromise due to parathyroid tumour apoplexy: an exceptionally rare and potentially life-threatening presentation, BMC Endocr, Disord. 17 (2017) 35, https://doi.org/10.1186/s12902-017-0186-2.

[22] H.U. Rehman, M. Markovski, A. Khalifa, Spontaneous cervical hematoma associated with parathyroid adenoma, CMAJ Can. Med. Assoc. J. J. Assoc. Medicale Can. 182 (2010), https://doi.org/10.1503/cmaj.091167 E632.
[23] A. Muñoz, N.J. Fischbein, J. de Vergas, J. Crespo, J. Alvarez-Vincent, Spontaneous retropharyngeal hematoma: diagnosis by mr imaging, AJNR Am. J. Neuroradiol. 22 (2001) 1209–1211.
[24] M. Bahl, A.R. Sepahdari, J.A. Sosa, J.K. Hoang, Parathyroid adenomas and hyperplasia on four-dimensional ct scans: three patterns of enhancement relative to the thyroid gland justify a three-phase protocol, Radiology 277 (2015) 454–462, https://doi.org/10.1148/radiol.2015142393.
[25] M. Goroshi, A.R. Lila, S.S. Jadhav, S. Sonawane, P. Hira, S. Goroshi, M.N. Garle, A. Dalvi, P. Sathe, T.R. Bandgar, N.S. Shah, Percentage arterial enhancement: an objective index for accurate identification of parathyroid adenoma/hyperplasia in primary hyperparathyroidism, Clin. Endocrinol. (Oxf.). 87 (2017) 791–798, https://doi.org/10.1111/cen.13406.
[26] W.A. Erdman, N.A. Breslau, J.C. Weinreb, P. Weatherall, H. Setiawan, R. Harrell, W. Snyder, Noninvasive localization of parathyroid adenomas: a comparison of X-ray computerized tomography, ultrasound, scintigraphy and MRI, Magn. Reson. Imaging 7 (1989) 187–194.
[27] G.H. Reference, Hyperparathyroidism-jaw Tumor Syndrome, Genet. Home Ref (accessed July 7, 2019), https://ghr.nlm.nih.gov/condition/hyperparathyroidism-jaw-tumor-syndrome.
[28] G.H. Reference, Parathyroid cancer, Genet. Home Ref (accessed July 7, 2019), https://ghr.nlm.nih.gov/condition/parathyroid-cancer.
[29] F. McClenaghan, Y.A. Qureshi, Parathyroid cancer, Gland Surg. 4 (2015) 329–338, https://doi.org/10.3978/j.issn.2227-684X.2015.05.09.
[30] Hannah du Preez, A. Adams, P. Richards, S. Whitley, Hyperparathyroidism jaw tumour syndrome: a pictorial review, Insights Imaging 7 (2016) 793–800, https://doi.org/10.1007/s13244-016-0519-0.
[31] R.H. Scott, C.A. Stiller, L. Walker, N. Rahman, Syndromes and constitutional chromosomal abnormalities associated with Wilms tumour, J. Med. Genet. 43 (2006) 705–715, https://doi.org/10.1136/jmg.2006.041723.
[32] K.J. Bradley, M.R. Hobbs, I.D. Buley, J.D. Carpten, B.M. Cavaco, J.E. Fares, P. Laidler, S. Manek, C.M. Robbins, I.S. Salti, N.W. Thompson, C.E. Jackson, R.V. Thakker, Uterine tumours are a phenotypic manifestation of the hyperparathyroidism-jaw tumour syndrome, J. Intern. Med. 257 (2005) 18–26, https://doi.org/10.1111/j.1365-2796.2004.01421.x.